Combined Mixed-Hybrid Finite Element–Finite Volume Scheme for Computation of Multicomponent Compressible Flow in Porous Media

O. Polívka and J. Mikyška

Abstract The paper deals with the numerical modeling of compressible single-phase flow of a mixture composed of several components in a porous medium. The mathematical model is formulated by Darcy's law, components continuity equations, constitutive relations, and initial and boundary conditions. The problem is solved numerically using a combination of the mixed-hybrid finite element method for the total flux discretization and the finite volume method for the discretization of the transport equations. The time discretization is carried out by Euler's method. The resulting large system of nonlinear algebraic equations is solved by the Newton-Raphson method. The dimensions of the obtained system of linear algebraic equations are significantly reduced so that they do not depend on the number of mixture components. The convergence of the numerical scheme is verified in the single-component case by comparing the numerical solution with an analytical solution.

1 Introduction

The mathematical modeling of the transport of multicomponent mixtures in the subsurface is important for many applications including oil recovery or CO_2 sequestration. The traditional approaches use either the fully implicit (fully coupled) method or a sequential method [5,14]. The fully implicit method is stable, allows for long time steps, but leads to extremely large systems of linear algebraic equations whose size is proportional to the number of mixture components. Alternatively, in sequential solution procedures like IMPEC (implicit pressure, explicit concentrations) [8], a pressure equation is formulated by summing up the transport equations

O. Polívka (✉) · J. Mikyška

Faculty of Nuclear Sciences and Physical Engineering, Department of Mathematics,
Czech Technical University in Prague, Trojanova 13, 120 00, Prague 2, Czech Republic
e-mail: ondrej.polivka@fjfi.cvut.cz; jiri.mikyska@fjfi.cvut.cz

[5, 14] or by another method [1, 7, 15]. This procedure allows the size of the solved system to be reduced, as only pressure is solved implicitly. However, this approach is conditionally stable and the time step has to be chosen prohibitively small in many cases.

In this paper, we improve our approach to the numerical modeling of the compressible multicomponent single-phase flow in a porous medium proposed in [13], where the numerical scheme was used for a simulation of methane injection into a propane reservoir. The original approach handled a velocity discretization; now, the total flux is discretized, and the convergence of the numerical to an analytical solution in a special case is verified. The scheme, based on a combination of the mixed-hybrid finite element method (MHFEM) and the finite volume method (FVM), has advantages of both the traditional sequential and implicit methods. As in the implicit schemes, our method leads to large systems of linear algebraic equations, but it is possible to reduce the size of the final system of equations to a size independent of the number of mixture components. Unlike in other sequential approaches, no pressure equation has to be formed as pressure is evaluated directly from the equation of state.

2   Mathematical Model

Let $\Omega \subset \mathbb{R}^2$ be a bounded domain with porosity ϕ [-], and (t_0, τ) be the time interval [s]. Consider the single-phase compressible flow of a fluid of n_c components in the domain at a constant temperature T [K]. Neglecting diffusion, the transport of the components is described by the following molar balance equations [7]

$$\frac{\partial(\phi c_i)}{\partial t} + \nabla \cdot (c_i \mathbf{v}) = f_i, \quad i = 1, \ldots, n_c, \tag{1}$$

$$c_i = c_i(\mathbf{x}, t), \quad \mathbf{x} \in \Omega, \ t \in (t_0, \tau),$$

$$\mathbf{q} = c\mathbf{v}, \quad c = \sum_{i=1}^{n_c} c_i, \tag{2}$$

where unknown quantities c_i, $i = 1, \ldots, n_c$, are the molar concentrations of the components [mol m^{-3}]. On the right hand side of Eq. (1), f_i [mol m^{-3} s^{-1}] denotes the sink/source term. The total molar flux $\mathbf{q}$ is expressed in (2) by the total molar concentration c and Darcy's velocity $\mathbf{v}$ [m s^{-1}] which is given according to [2] by

$$\mathbf{v} = -\mu^{-1} \mathsf{K}(\nabla p - \varrho \mathbf{g}). \tag{3}$$

In (3), K is the medium intrinsic permeability [m^2] (generally symmetric and uniformly positive-definite tensor), μ is the viscosity [kg m^{-1} s^{-1}], ∇p denotes a gradient of the pressure p [Pa], $\mathbf{g}$ is the gravitational acceleration vector [m s^{-2}], and

ϱ is the fluid density [$\mathrm{kg\,m^{-3}}$]. Equations (1) and (3) are coupled with constitutive relations expressing dependencies (to be found in [6, 10, 12, 13])

$$p = p\left(c_1, \ldots, c_{n_c}, T\right), \quad \varrho = \varrho\left(c_1, \ldots, c_{n_c}\right), \quad \mu = \mu\left(c_1, \ldots, c_{n_c}, T\right). \quad (4)$$

The initial and boundary conditions are given by

$$c_i(\mathbf{x}, t_0) = c_i^0(\mathbf{x}), \qquad \mathbf{x} \in \Omega, \ i = 1, \ldots, n_c, \tag{5a}$$

$$c_i(\mathbf{x}, t) = c_i^D(\mathbf{x}, t), \qquad \mathbf{x} \in \Gamma_c(t), \ t \in (t_0, \tau), \ i = 1, \ldots, n_c, \tag{5b}$$

$$p(\mathbf{x}, t) = p^D(\mathbf{x}, t), \qquad \mathbf{x} \in \Gamma_p, \ t \in (t_0, \tau), \tag{5c}$$

$$\mathbf{q}(\mathbf{x}, t) \cdot \mathbf{n}(\mathbf{x}) = q^N(\mathbf{x}, t), \qquad \mathbf{x} \in \Gamma_q, \ t \in (t_0, \tau), \tag{5d}$$

where $\mathbf{n}$ is the unit outward normal vector to the boundary $\partial\Omega$, $\Gamma_p \cup \Gamma_q = \partial\Omega$, and $\Gamma_p \cap \Gamma_q = \emptyset$. Further, $\Gamma_c(t)$ denotes the inflow part of the boundary $\partial\Omega$ at time t, i.e. $\Gamma_c(t) = \left\{\mathbf{x} \in \partial\Omega \mid \mathbf{q}(\mathbf{x}, t) \cdot \mathbf{n}(\mathbf{x}) < 0\right\}$. On $\Gamma_c \cap \Gamma_p$, values of $c_i^D, i = 1, \ldots, n_c$, are constrained by Eqs. (4) and (5c) so that $p^D = p\left(c_1^D, \ldots, c_{n_c}^D, T\right)$.

3   Numerical Scheme

The system of Eqs. (1)–(5) is solved numerically by a combination of the MHFEM, for total flux relation (2), and the FVM, for transport Eqs. (1). We consider a 2D polygonal domain Ω with the boundary $\partial\Omega$ which is covered by a conforming triangulation T_Ω. Let us denote K the element of the mesh T_Ω with area $|K|$, E the edge of an element with the length $|E|$, n_k the number of elements of the triangulation, and n_e the number of edges of the mesh.

Discretization of the Total Molar Flux   Unlike in [13], where the velocity $\mathbf{v}$ was discretized, here, the total molar flux $\mathbf{q}$ is approximated in the Raviart-Thomas space of the lowest order (RT_K^0) over the element $K \in T_\Omega$ as

$$\mathbf{q} = \sum_{E \in \partial K} q_{K,E} \mathbf{w}_{K,E}, \tag{6}$$

where the coefficient $q_{K,E}$ is the numerical flux of vector function $\mathbf{q}$ through the edge E of the element K with respect to outer normal, and $\mathbf{w}_{K,E}$ represents the piecewise linear RT_K^0-basis function associated with the edge E (see [3, 4, 11, 13]).

If we express the pressure gradient from Darcy's law (3), multiply both sides of the obtained relation by the basis function $\mathbf{w}_{K,E}$, integrate over K, use (6) and properties of the RT_K^0 space, we derive a discrete form of (2) and (3)

$$q_{K,E} = c_K \mu_K^{-1}\left(\alpha_{K,E}\, p_K - \sum_{E' \in \partial K} \beta_{K,E,E'}\, p_{K,E'} + \gamma_{K,E}\varrho_K\right), \quad E \in \partial K. \tag{7}$$

Green's theorem and the mean value theorem were also employed in the derivation
[13]. In (7), $\alpha_{K,E}, \beta_{K,E,E'}$, and $\gamma_{K,E}$ are coefficients dependent on the mesh
geometry and on the local values of permeability (details in [13]); p_K is the cell
pressure average, $p_{K,E'}$ is the edge pressure average, and μ_K, ϱ_K denote the mean
values of viscosity and density over the cell K, respectively.

The continuity of the flux and pressure on the edge E between neighboring
elements $K, K' \in T_\Omega$ can be written as

$$q_{K,E} + q_{K',E} = 0, \quad p_{K,E} = p_{K',E} =: p_E. \tag{8}$$

Boundary conditions (5c) and (5d) in a discrete form read as

$$p_{K,E} = p^D(E), \quad \forall E \subset \Gamma_p, \tag{9a}$$

$$q_{K,E} = q^N(E), \quad \forall E \subset \Gamma_q, \tag{9b}$$

where $p^D(E)$ is the prescribed value of the pressure p averaged on the edge E, and
$q^N(E)$ is prescribed flux through the edge E.

The numerical fluxes can be eliminated by substituting $q_{K,E}$ from (7) into (8) and
(9b). For further derivation, let us consider time dependent quantities at time t_{n+1}
denoted by upper index $n + 1$. Then, Eqs. (7)–(9) transform to the following system
of n_e linear algebraic equations

$$F_E \equiv \begin{cases} \displaystyle\sum_{K:E\in\partial K} c_K^{n+1} \left(\mu_K^{n+1}\right)^{-1} \left(\alpha_{K,E} p_K^{n+1} - \sum_{E'\in\partial K} \beta_{K,E,E'} p_{K,E'}^{n+1} + \gamma_{K,E} \varrho_K^{n+1}\right) \\ \qquad\qquad\qquad\qquad - \displaystyle\sum_{K:E\in\partial K\cap\Gamma_q} q^N(E) = 0, \quad \forall E \not\subset \Gamma_p, \\ p_{K,E}^{n+1} - p^D(E) = 0, \quad \forall E \subset \Gamma_p. \end{cases} \tag{10}$$

Herein, $\sum_{K:E\in\partial K}$ denotes the sum over the elements adjacent to the edge E.

Approximation of the Transport Equations Transport Eqs. (1) with the initial
and boundary conditions (5) are discretized by the FVM [9]. Equation (1) is
then integrated over an arbitrary element K. Using Green's theorem, applying the
mean value theorem, and denoting $\phi_K, c_{i,K}, f_{i,K}$, the averaged values of ϕ, c_i, f_i
$(i = 1, \ldots, n_c)$ over the cell K, respectively, the discrete form of (1) reads as

$$\frac{d(\phi_K c_{i,K})}{dt}|K| + \sum_{E\in\partial K} \widetilde{z_{i,E}} \int_E \mathbf{q} \cdot \mathbf{n}_{K,E} = f_{i,K}|K|, \tag{11}$$

where $\widetilde{z_{i,E}}$ denotes the mole fraction $z_i = c_i/c$ of the i-th component on the edge
E, and $\mathbf{q}$ is given by (2). The integral in (11) is equal to the numerical flux $q_{K,E}$.

Let us suppose that the porosity does not depend on time. The time derivative
of $c_{i,K}$ in (11) is approximated by the time difference with a time step Δt_n. Using
Euler's method [9], we obtain for every n, all $K \in T_\Omega$, and $i = 1, \ldots, n_c$

$$F_{K,i} \equiv \phi_K |K| \frac{c_{i,K}^{n+1} - c_{i,K}^n}{\Delta t_n} + \sum_{E \in \partial K} \widetilde{z_{i,E}}^n \, q_{K,E}^{n+1} \left(p_{K,E}^{n+1}, c_{1,K}^{n+1}, \dots, c_{n_c,K}^{n+1} \right) - f_{i,K} |K| = 0,$$

(12)

where $q_{K,E}^{n+1}$ is given by (7). The value of $\widetilde{z_{i,E}}^n$ is chosen by upwinding as

$$\widetilde{z_{i,E}}^n = \begin{cases} z_{i,K}^n & \text{for} \quad q_{K,E}^{n+1} \geq 0, \\ z_{i,K'}^n & \text{for} \quad q_{K,E}^{n+1} < 0 \land E \not\subset \partial \Omega : K \cap K' = E, \\ z_{i,E}^{D,n} & \text{for} \quad q_{K,E}^{n+1} < 0 \land E \subset \partial \Omega, \end{cases}$$

(13)

where z_i^D represents the mole fraction of the i-th component on the inflow boundary computed from (5b). Note that the scheme is almost fully implicit, the only term in (12) which is evaluated explicitly is the value of $\widetilde{z_{i,E}}^n$.

The initial and boundary conditions (5a) and (5b) are approximated as

$$c_{i,K}^0 = c_i^0(K), \qquad \forall K \in T_\Omega, \ i = 1, \dots, n_c,$$ (14a)

$$\widetilde{z_{i,E}}^n = z_i^D(E, t_n), \qquad \forall E \subset \Gamma_c(t), \ i = 1, \dots, n_c, \ t_0 < t_n < \tau.$$ (14b)

Combining the MHFEM and FVM Schemes Let us denote F_E and $F_{K,i}$, for edge $E \in \{1, \dots, n_e\}$, element $K \in \{1, \dots, n_k\}$, and component $i \in \{1, \dots, n_c\}$, the left hand sides of Eqs. (10) and (12) with $q_{K,E}^{n+1}$ substituted from relation (7). The cell-averaged values $p_K = p\left(c_{1,K}, \dots, c_{n_c,K}\right)$, $\varrho = \varrho_K\left(c_{1,K}, \dots, c_{n_c,K}\right)$, and $\mu_K = \mu\left(c_{1,K}, \dots, c_{n_c,K}\right)$ are evaluated using (4). The system of $n_e + n_k \times n_c$ equations

$$\mathbf{F} = \left[F_1, \dots, F_{n_e}; F_{1,1}, \dots, F_{1,n_c}, \dots, F_{n_k,1}, \dots, F_{n_k,n_c} \right]^T = \mathbf{0}$$

for unknown molar concentrations $c_{1,K}^{n+1}, \dots, c_{n_c,K}^{n+1}$, $K \in \{1, \dots, n_k\}$, and edge-averaged pressures p_E^{n+1}, $E \in \{1, \dots, n_e\}$, is a nonlinear system of algebraic equations which we solve using the Newton-Raphson method (NRM). The resulting system of linear algebraic equations is shown in Fig. 1, where the sparse Jacobi matrix is unsymmetric, and the unknown vector is represented by corrections of molar concentrations and edge pressures. The nonzero black-colored blocks in Fig. 1 are given by partial derivatives

$$\left(\mathbf{J}_K\right)_{i,j} = \frac{\partial F_{K,i}}{\partial c_{j,K}^{n+1}} \,, \quad \left(\mathbf{J}_{K,E}\right)_i = \frac{\partial F_{K,i}}{\partial p_{K,E}^{n+1}} \,, \quad \left(\mathbf{J}_{E,K}\right)_j = \frac{\partial F_E}{\partial c_{j,K}^{n+1}} \,, \quad J_{E,E'} = \frac{\partial F_E}{\partial p_{K,E'}^{n+1}} \,,$$

(15)

where $J_{E,E'}$ is element of $\mathbf{J}_{E,E'}$ and $i, j = 1, \dots, n_c$; $K = 1, \dots, n_k$; $E, E' = 1, \dots, n_e$. The partial derivatives in (15) can be evaluated analytically using (4), (10), and (12).
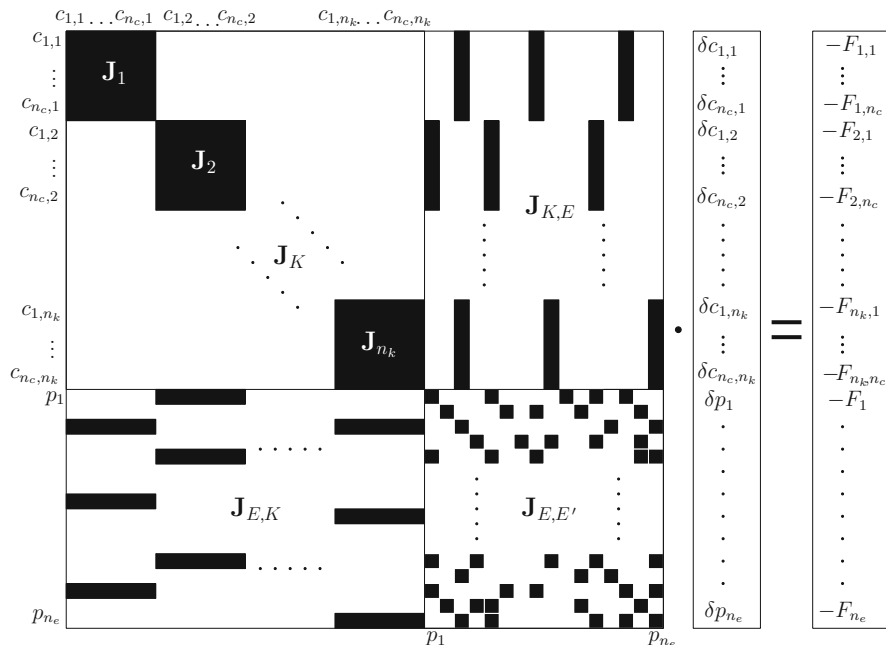
Fig. 1 Structure of the system of linear algebraic equations in the NRM

The size of the system in Fig. 1 can be reduced by inverting the $\mathbf{J}_K$ blocks for all K (the inversion is possible since the blocks are diagonally dominant for small time steps) and eliminating vectors $\mathbf{J}_{E,K}$ for all E, K. Thus, we derive a reduced system of n_e equations for n_e corrections of pressures δp_E with the same structure as $\mathbf{J}_{E,E'}$. Once δp_E are computed, corrections of concentrations $\delta c_{1,K}, \ldots, \delta c_{n_c,K}$ on each cell K can be evaluated by the back-substitution utilizing the $\mathbf{J}_K$ inversions.

4 Experimental Analysis of Convergence

In this section, we verify convergence of the proposed scheme using the experimental convergence analysis. Choosing $n_c = 1$, $\phi = 1$, $f = 0$, $\mathbf{g} = 0$, $\mathsf{K} = 1$, $\mu = 0.5$, and $p = c$, Eqs. (1) and (3) transform to

$$\frac{\partial c}{\partial t} + \nabla \cdot (c\mathbf{v}) = 0, \quad \mathbf{v} = -2\,\nabla c. \tag{16}$$

We set the initial and boundary conditions as follows

$$c(\mathbf{x}, t_0) = B_2(x, t_0), \qquad \mathbf{x} \in \Omega, \qquad\qquad (17\text{a})$$

$$p(\mathbf{x}, t) = B_2(x, t), \qquad \mathbf{x} \in \Gamma_p, \ t \in (t_0, \tau), \qquad (17\text{b})$$

$$\mathbf{q}(\mathbf{x}, t) \cdot \mathbf{n}(\mathbf{x}) = 0, \qquad \mathbf{x} \in \Gamma_q, \ t \in (t_0, \tau), \qquad (17\text{c})$$

where $B_2(x, t)$ is the Barenblatt solution of (16) prescribed by

$$B_m(x, t) = t^{-k} \left[\left(1 - \frac{k(m-1)}{2m} \frac{|x|^2}{t^{2k}} \right)_+ \right]^{1/(m-1)}, \quad m = 2, \qquad (18)$$

where $c_+ = \max(c, 0)$ and $k = (m + 1)^{-1}$. For any time $t > 0$, solution (18) has a compact support $[-t^k \sqrt{2m/(k(m-1))}, \ t^k \sqrt{2m/(k(m-1))}]$ becoming wider in a finite speed [16].

Using the numerical scheme derived in Sect. 3, we solve Eqs. (16) and (17) in a rectangular domain $100 \times 20\,\text{m}^2$, where Γ_p is composed of line segments $x = 0$ and $x = 100$ ($0 \leq y \leq 20$), while Γ_q contains the rest of the boundary $\partial\Omega$, i.e. the horizontal and vertical boundary $y = 0$ and $y = 20$. Both parts of Γ_p are outflow boundaries, thus $\Gamma_c = \emptyset$. The initial time $t_0 = 10^4\,$s and the final time $\tau = 10^6\,$s.

The numerical solution is compared with the analytical one (18) by means of the experimental orders of convergence (EOCs). Every numerical (element-wise constant) solution is computed on a homogeneous regular triangular grid containing $n = 2 \times n_x \times n_y$ triangles, and projected to a grid on which the analytical solution is computed. The analytical solution is element-wise linear by evaluating from (18) three values on edges of each element. Error E_n between the analytical solution and the projection of the numerical solution (to the grid of the analytical solution) originally computed on the grid n in three consistent norms L^1, L^2, and L^∞ is evaluated.

In Table 1, EOCs and errors of concentration on five grids with $n_x = n_y$ and the finest $n_x = 320$ are included. The analytical solution is interpolated on the grid $n_x = 640$. The time step for the solution $n_x = 320$ is chosen constant $\Delta t = 386.7\,$s. On every coarser grid, Δt is four times larger with each mesh refinement (i.e. $\Delta t \sim 1/n$) to observe EOC of the space discretization.[1]

The numerical solutions computed on the grids with a different n_x and n_y are compared with the analytical solution interpolated on the grid of $2 \times 1{,}600 \times 320$ cells in Table 2. Again, Δt is four times larger with each mesh refinement (i.e. $\Delta t \sim 1/n$)[1], $\Delta t = 386.7\,$s for the numerical solution with $n = 2 \times 800 \times 160$.

---

[1]For $\Delta t \sim 1/\sqrt{n}$ all EOCs equal to 1 were observed in L^1 and L^2 norms, and the error of the time discretization, thus, prevailed.

Table 1 EOCs and errors of concentration c at time $\tau = 10^6$ s compared with the analytical solution on the grid $n_x = 640$ ($n = 2 \times n_x \times n_x$ elements) and the time step $\Delta t = 386.7$ s for the numerical solution $n_x = 320$. On coarser grids, $\Delta t \sim 1/n$

Grid (n)	$\|E_n\|_1$	EOC$_1$	$\|E_n\|_2$	EOC$_2$	$\|E_n\|_\infty$	EOC$_\infty$
$2 \times 20 \times 20$	2.5113×10^{-2}		6.1743×10^{-4}		2.8684×10^{-5}	
		1.8297		1.7739		1.1119
$2 \times 40 \times 40$	7.0646×10^{-3}		1.8055×10^{-4}		1.3271×10^{-5}	
		1.4607		1.3506		1.0817
$2 \times 80 \times 80$	2.5667×10^{-3}		7.0798×10^{-5}		6.2704×10^{-6}	
		1.2083		1.1165		1.1570
$2 \times 160 \times 160$	1.1108×10^{-3}		3.2653×10^{-5}		2.8119×10^{-6}	
		1.1040		1.0319		1.3770
$2 \times 320 \times 320$	5.1678×10^{-4}		1.5969×10^{-5}		1.0827×10^{-6}	

Table 2 EOCs and errors of concentration c at time $\tau = 10^6$ s compared with the analytical solution on the grid $n = 2 \times 1,600 \times 320$ and the time step $\Delta t = 386.7$ s for the numerical solution $n = 2 \times 800 \times 160$. On coarser grids, $\Delta t \sim 1/n$

Grid (n)	$\|E_n\|_1$	EOC$_1$	$\|E_n\|_2$	EOC$_2$	$\|E_n\|_\infty$	EOC$_\infty$
$2 \times 50 \times 10$	2.3185×10^{-2}		5.675×10^{-4}		1.8943×10^{-5}	
		2.0520		2.0493		1.7276
$2 \times 100 \times 20$	5.5911×10^{-3}		1.3711×10^{-4}		5.7199×10^{-6}	
		1.8051		1.7690		1.1810
$2 \times 200 \times 40$	1.5999×10^{-3}		4.0231×10^{-5}		2.5228×10^{-6}	
		1.5337		1.4358		1.1608
$2 \times 400 \times 80$	5.5262×10^{-4}		1.4871×10^{-5}		1.1283×10^{-6}	
		1.2957		1.1655		1.3789
$2 \times 800 \times 160$	2.2510×10^{-4}		6.6297×10^{-6}		4.3386×10^{-7}	

5   Conclusion

In this work, we have developed a numerical scheme based on a combination of the MHFEM and FVM for simulation of single-phase compressible multicomponent flow in a porous medium. We proposed a technique reducing significantly the system into a size that is independent of the number of mixture components. Consequently, computational costs are comparable with the traditional sequential approaches. Our method provides an exact local mass balance (up to the non-linear solver error) which is important for solving problems especially in a heterogeneous medium. Convergence of the numerical scheme was verified by evaluating EOCs in a special case of the problem for which an analytical solution is known. The EOCs range from 1.03 to 2.05 behaving similarly in both examined cases.

References

1. Acs, G., Doleschall, S., Farkas, E.: General Purpose Compositional Model, *Society of Petroleum Engineers Journal*, Vol.: 25, Issue: 4 (1985) 543–553.
2. Bear, J., Verruijt, A.: Modeling Groundwater Flow and Pollution (1987), D. Reidel Publishing Company, Dordrecht, Holland.
3. Brezzi, F., Fortin, M.: Mixed and Hybrid Finite Element Methods (1991), Springer-Verlag, New York Inc.
4. Chavent, G., Roberts, J. E.: A unified physical presentation of mixed, mixed-hybrid finite elements and standard finite difference approximations for the determination of velocities in waterflow problems, *Advances in Water Resources*, 14(6) (1991).
5. Chen, Z., Huan, G., Ma, Y.: Computational Methods for Multiphase Flows in Porous Media (2006), SIAM, Philadelphia.
6. Holzbecher, E. O.: Modeling Density-Driven Flow in Porous Media: Principles, Numerics, Software (1998), Springer-Verlag, Berlin.
7. Hoteit, H., Firoozabadi, A.: Multicomponent Fluid Flow by Discontinuous Galerkin and Mixed Methods in Unfractured and Fractured Media, *Water Resources Research* (2005), 41, W11412, doi:10.1029/2005WR004339.
8. Huyakorn, P. S., Pinder, G. F.: Computational Methods in Subsurface Flow (1983), Academic Press, Inc., New York.
9. Leveque, R. J.: Finite Volume Methods for Hyperbolic Problems (2002), Cambridge University Press, Cambridge.
10. Lohrenz, J., Bray, B. G., Clark, C. R.: Calculating Viscosities of Reservoir Fluids From Their Compositions, *Journal of Petroleum Technology* Oct. (1964) 1171–1176.
11. Mikyška, J., Firoozabadi, A.: Implementation of higher-order methods for robust and efficient compositional simulation, *Journal of Computational Physics* 229 (2010) 2898–2913.
12. Peng, D. Y., Robinson, D. B.: A New Two-Constant Equation of State, *Industrial and Engineering Chemistry: Fundamentals 15* (1976) 59–64.
13. Polívka O., Mikyška J.: Numerical simulation of multicomponent compressible flow in porous medium, *Journal of Math-for-Industry* Vol. 3 (2011C-7), (2011) 53–60.
14. Russel, T. F., Wheeler, M. F.: Finite Element and Finite Difference Methods for Continuous Flows in Porous Media in: *The Mathematics of Reservoir Simulation, Frontiers in Applied Mathematics* (1983) 35–106, SIAM, Philadelphia.
15. Young, L. C., Stephenson, R. E.: A Generalized Compositional Approach for Reservoir Simulation, *Society of Petroleum Engineers Journal*, Vol.: 23, Issue: 5 (1983) 727–742.
16. Zhang, Q., Wu, Z.-L.: Numerical Simulation for Porous Medium Equation by Local Discontinuous Galerkin Finite Element Method, *Journal of Scientific Computing* (2009) 38: 127–148, DOI 10.1007/s10915-008-9223-7.